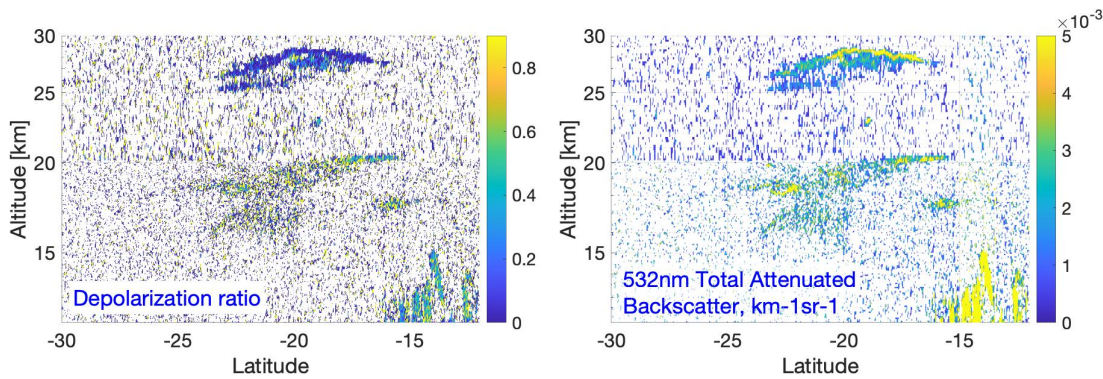


1 Supplementary Information

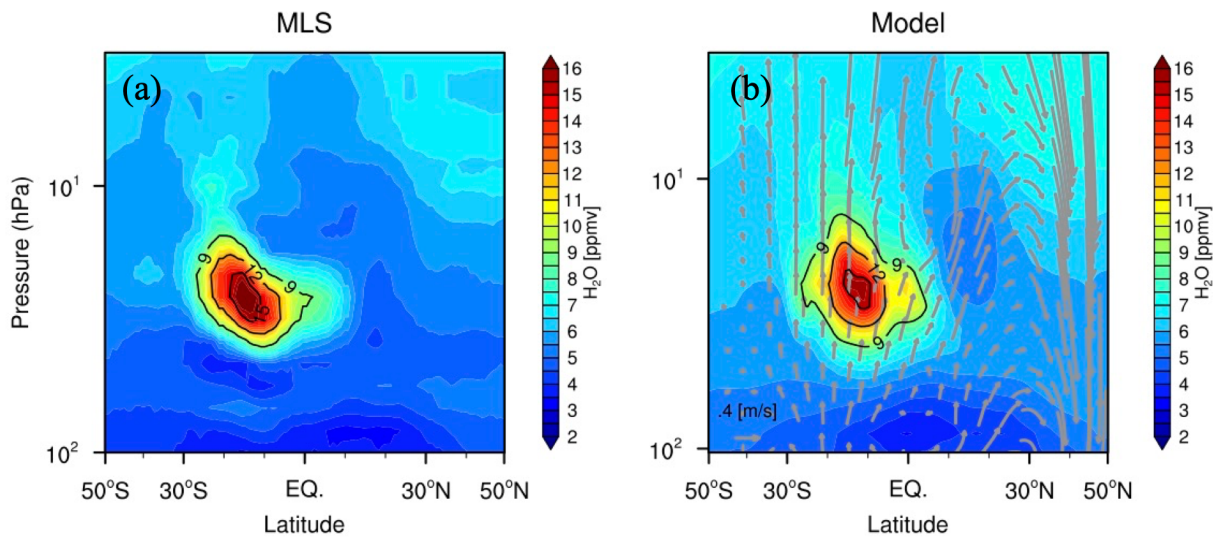
2 **Perturbations in stratospheric aerosol evolution due to the water-rich**  
3 **plume of the 2022 Hunga-Tonga eruption**

4 Zhu et al.

5



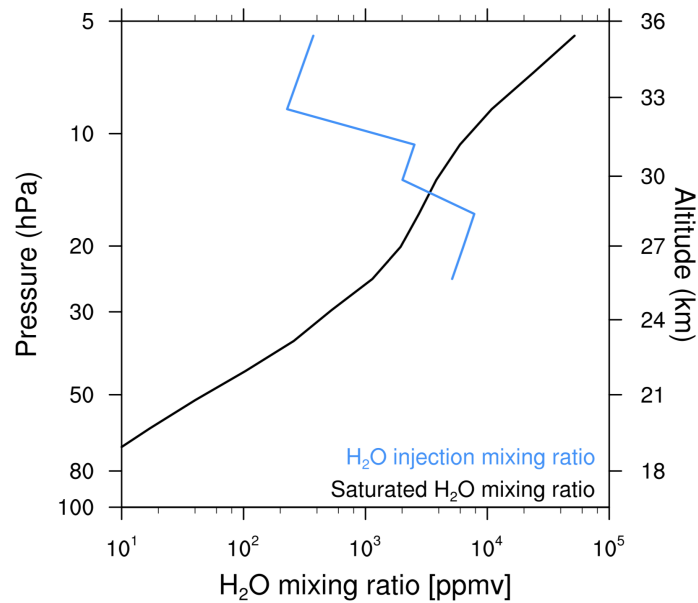
7 **Supplementary Figure 1. The CALIPSO observation on Jan 16.** The left panel is the  
8 depolarization ratio showing the plume at 30 km with small depolarization and the plume at 20  
9 km with large depolarization. The right panel shows the backscatter coefficient.  
10



12 **Supplementary Figure 2. Zonal average H<sub>2</sub>O comparisons between MLS and the model**  
13 **simulation.** Zonal average H<sub>2</sub>O from MLS v4 data on March 1 (a) and the SO<sub>2</sub>\_H<sub>2</sub>O case with

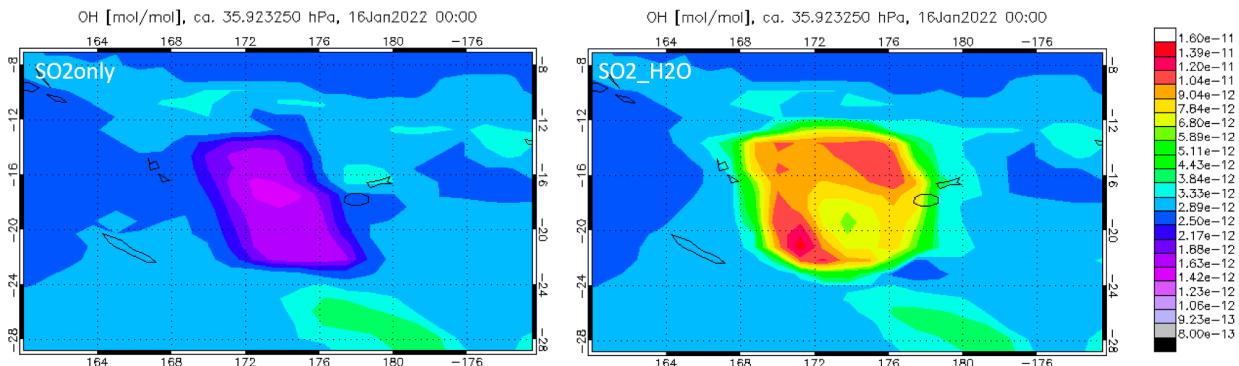
14 Brewer-Dobson circulation (vectors) superimposed on March 1 (b). The simulation shows a  
 15 positive bias in the background because WACCM generally has a wet bias in the stratosphere  
 16 compared to MLS<sup>1</sup>.

17  
 18



19  
 20 **Supplementary Figure 3. The H<sub>2</sub>O injection scheme relative to the H<sub>2</sub>O saturation ratio in**  
 21 **the stratosphere.** The black line is the saturated H<sub>2</sub>O mixing ratio near HTHH on Jan 15 based  
 22 on the model nudged GEOS5 temperature profile and the temperature profile at the Fiji radiosonde  
 23 station using the vapor pressure equation of Goff & Gratch<sup>2</sup>. The blue line is the mixing ratio of  
 24 H<sub>2</sub>O injection assuming all H<sub>2</sub>O is in the vapor phase in the H2O\_SO2 case near HTHH on Jan 15.  
 25 The figure shows water vapor is saturated at pressures above 15 hPa where ice forms.

26  
 27



28  
 29 **Supplementary Figure 4. The OH concentration at 35 hPa after the eruption.** The left panel  
 30 without water injection shows the OH gets depleted in the SO<sub>2</sub> plume. The right panel with water  
 31 injection shows H<sub>2</sub>O converting to OH rapidly inside the plume.

32

33

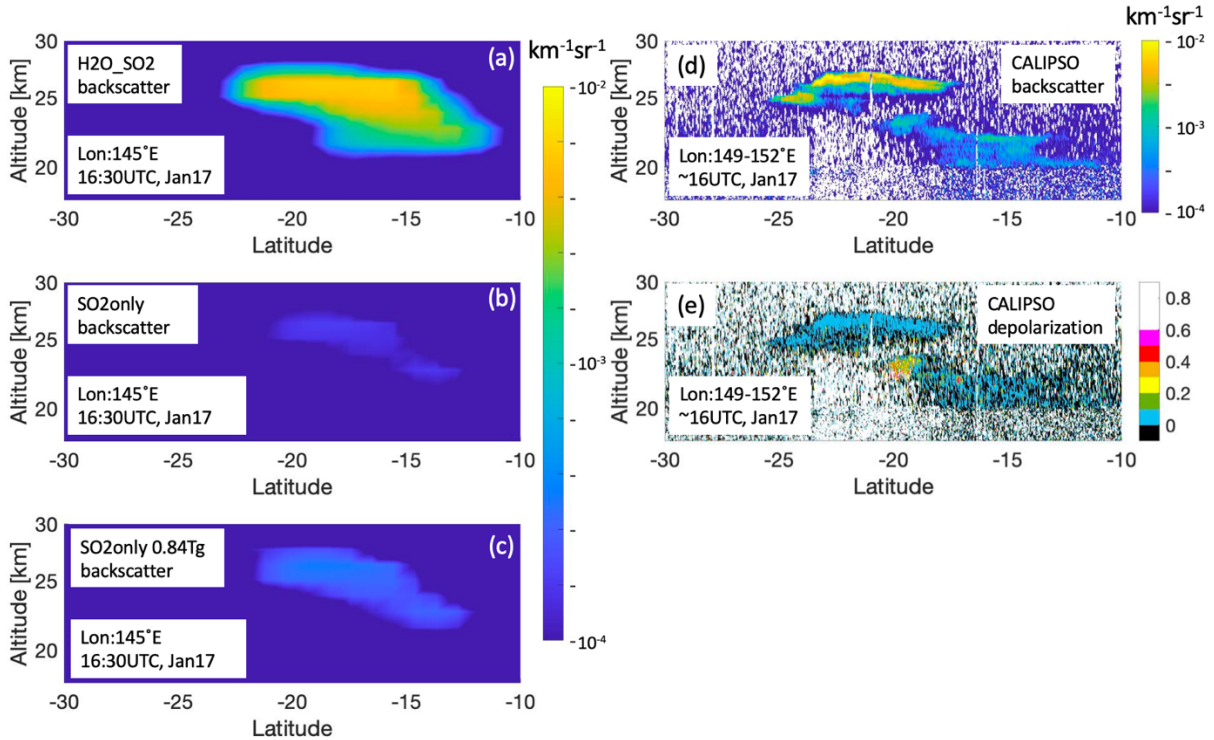
34 **Supplementary Note 1**

35

36 In this paragraph, we compare several model simulations with various injection amount  
37 and latitude bands to choose the best simulation cases.

38 Figure S5b shows that the H2O\_SO2 case explains the CALIPSO backscatter. Without  
39 water injection, even doubling the injection for the SO2 case cannot create large extinction for  
40 the first month as shown in Figure S5c. CALIPSO shows the backscatter peaks about  $1e^{-3}$  to  $1e^{-2}$   
41  $km^{-1}sr^{-1}$  near 25 km (Figure S5d), which can be reproduced by the SO2\_H2O case (Figure S5a).  
42 While the SO2only case with 0.42 injection (Figure S5b) only peaks at about  $2e^{-4} km^{-1}sr^{-1}$ ;  
43 doubling the SO2only case injection (0.84Tg) peaks at about  $4e^{-4} km^{-1}sr^{-1}$  (Figure S5c).

44 Therefore, the SO2\_H2O case is better than the SO2only case because the water injection is  
45 needed for immediately creating high extinction aerosol layers as observed by both OMPS  
46 (Figure 3) and CALIPSO, which is similar to a hypothetical experiment done by LeGrande et al.  
47 <sup>3</sup> that simulates the Pinatubo sized eruption with  $\sim 150$  Tg of water injection.  
48

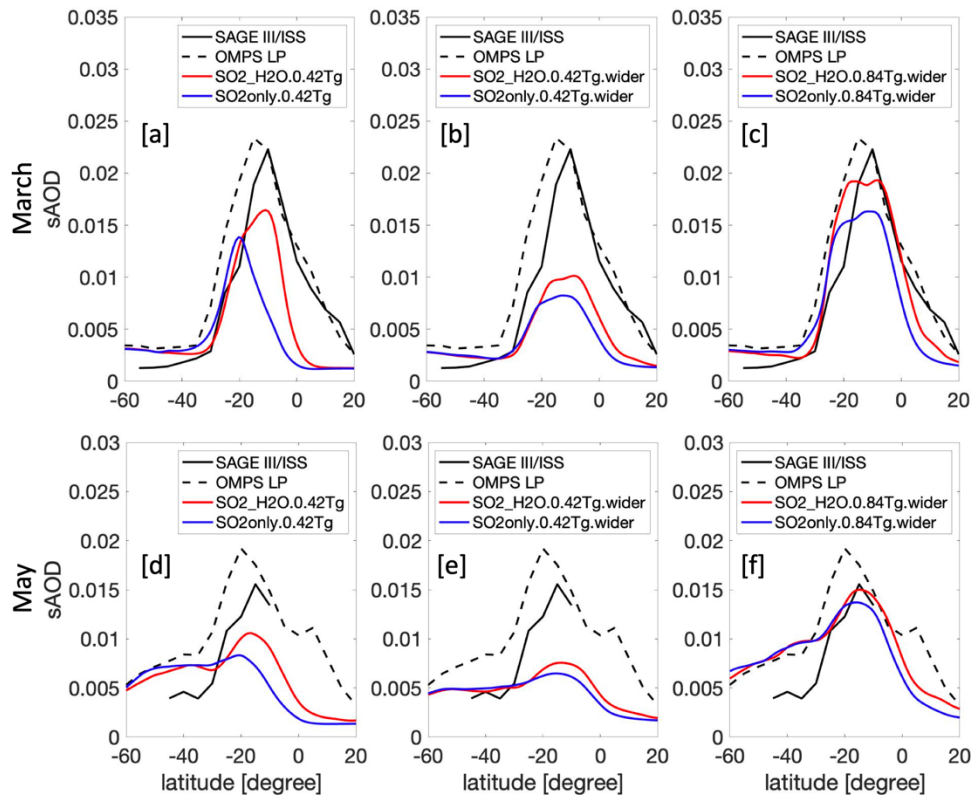


49

50 **Supplementary Figure 5. The backscatter coefficient comparisons between several model**  
51 **cases and CALIPSO.** CALIOP backscatter coefficient at 532 nm (d) compared with the  
52 simulation on Jan 17  $\sim 16$  UTC along CALIOP track: a) 0.42 Tg SO2\_H2O case, b) 0.42 Tg  
53 SO2only case and c) 0.84 Tg SO2only case. Simulated aerosol backscatter is calculated using the  
54 simulated visible extinction coefficient divided by the extinction-to-backscatter ratio (value = 55  
55 sr) for volcanic sulfate suggested by the Wyoming balloon particle counter data calculation two  
56 years after the Mt. Pinatubo eruption in 1993 (value  $\sim 50$  sr)<sup>4,5</sup> and CALIOP lidar ratio retrievals  
57 for sulfate-rich aerosol layer (value = 60 sr)<sup>6</sup>. e) CALIOP depolarization ratio shows low

58 depolarization for both plumes, but the lower plume shows a small segment of high  
 59 depolarization near 23 km and 20°S.  
 60

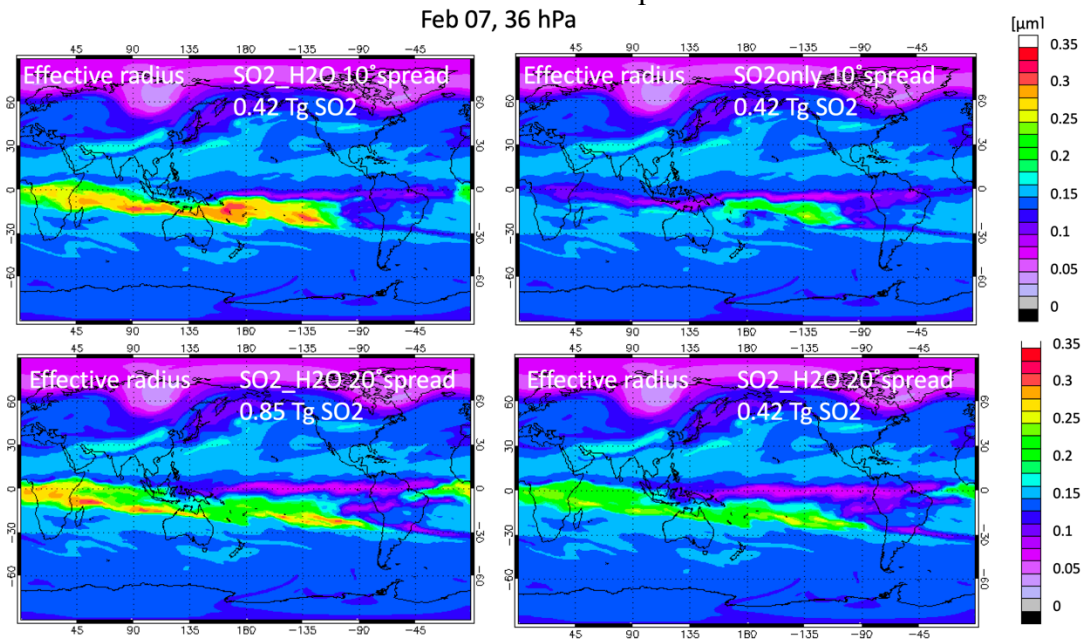
61 Another issue with the model is that the area covered by the cloud is larger than in the  
 62 model. Figure S6 shows sAOD averaged over March and May from SAGE III/ISS and OMPS.  
 63 SO<sub>2</sub>\_H<sub>2</sub>O cases always produce higher sAOD than the SO<sub>2</sub>only cases for the same injection  
 64 scenarios. If we injection in a 10-degree latitude band (S6a and S6d) with 0.42 Tg of SO<sub>2</sub>, we get  
 65 a smaller sAOD near tropics and NH, but SH mid-latitude compares with OMPS well. If we  
 66 injection in a 20-degree latitude band (S6b and S6e) with 0.42 Tg of SO<sub>2</sub>, the sAOD is significantly  
 67 reduced. The model matches the observation the best when injecting 0.84 Tg of SO<sub>2</sub> into 20-degree  
 68 latitude bands (S6c and S6f).



69  
 70 **Supplementary Figure 6. zonal average sAOD in March and May from OMPS, SAGE III-**  
 71 **ISS, and several model cases.** The black line is from SAGE III/ISS, the dashed black line is from  
 72 OMPS LP. The red color is SO<sub>2</sub>\_H<sub>2</sub>O cases with various injection amounts and injection widths;  
 73 the blue color is the SO<sub>2</sub>only case. In panels b, c, e, and f, the modeled injection latitude bands  
 74 double the original injection latitude bands.  
 75

76 Artificially injecting into a 20-degree band can cause changes in the initial microphysics,  
 77 resulting in smaller effective radii of particles and smaller optical depths. As stated in Murphy et  
 78 al.<sup>7</sup>, sulfate particles with a radius around 0.3 μm give the largest extinction for a given mass. This  
 79 can be one of the reasons why we need to double the injection to produce observed sAOD. Figure  
 80 S7 shows the effective radius from several model runs. We can see the SO<sub>2</sub>\_H<sub>2</sub>O case has the  
 81 effective radius of 0.3 μm. If we spread the plume wider, the effective radius is reduced to 0.2 μm.

82 If we spread the plume wider and increase the injection to 0.84 Tg, the effective radius is closer to  
83 0.3  $\mu\text{m}$ . OMPS clearly shows the plume spreading fast from 10 degrees wide to 30 degrees wide  
84 during the first couple of weeks, which could be caused by localized sub-grid winds due to the  
85 volcanic debris that the model does not have the spatial resolution to simulate.



86  
87 **Supplementary Figure 7. The effective radius of the particles from several model runs.**  
88

89 Based on our current best knowledge of  $\text{SO}_2$  injection: Carn et al.<sup>8</sup> summarized the  
90 estimation as about 0.4-0.5 Tg. However, our model produces the best match to optical data with  
91 the 0.84 Tg injection with 20-degree latitude band injection. Our current model setting is the best  
92 estimation of injection area and injection amount of  $\text{SO}_2$  and  $\text{H}_2\text{O}$  based on observations. However,  
93 there could be ways to remove this conflict in the future. For example, small ash particles coated  
94 with sulfate could increase the extinction for a smaller  $\text{SO}_2$  injection and still be round allowing  
95 them to not depolarize and conflict with CALIPSO data. Ash particles can have a small density  
96 which allows particles to be moderately large and still persist without falling<sup>9</sup>.

97

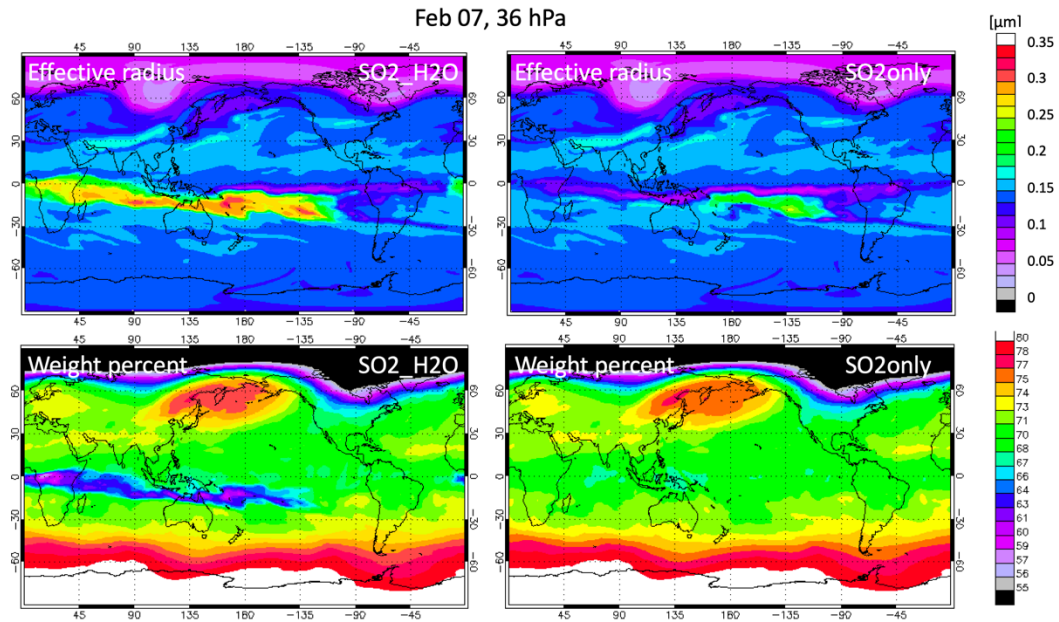
98

99

100

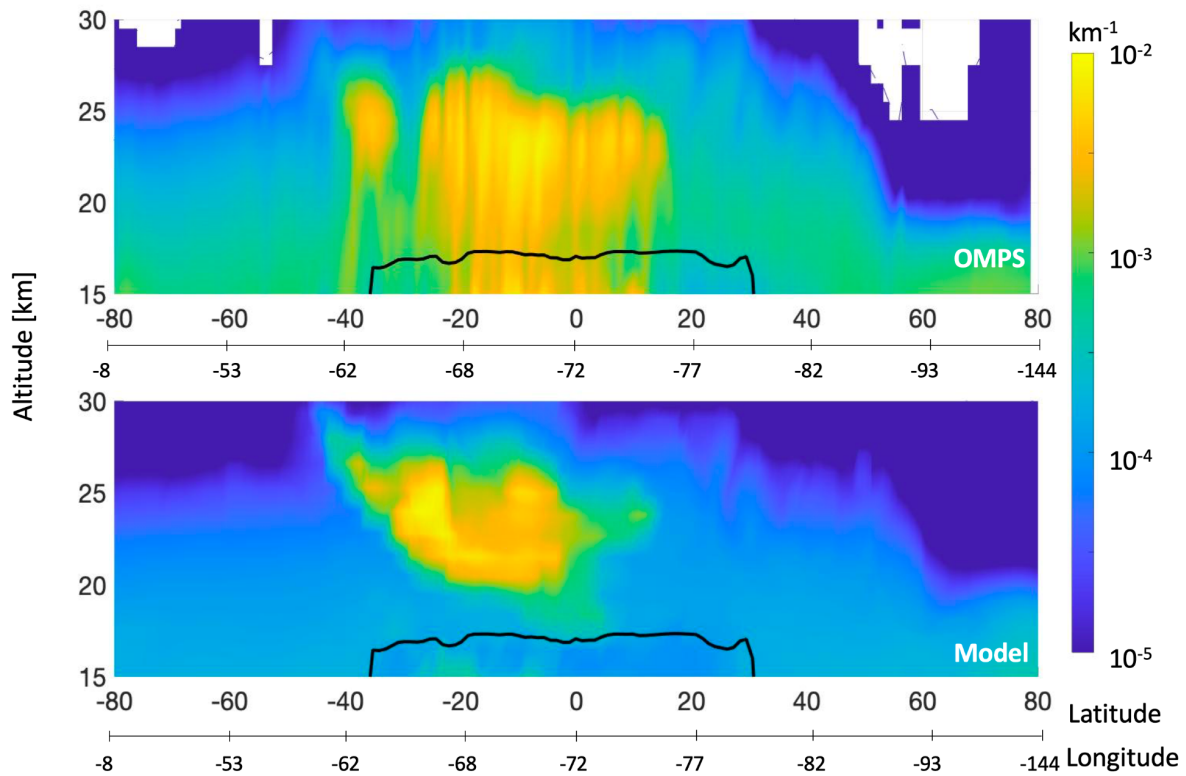
101

102  
103  
104

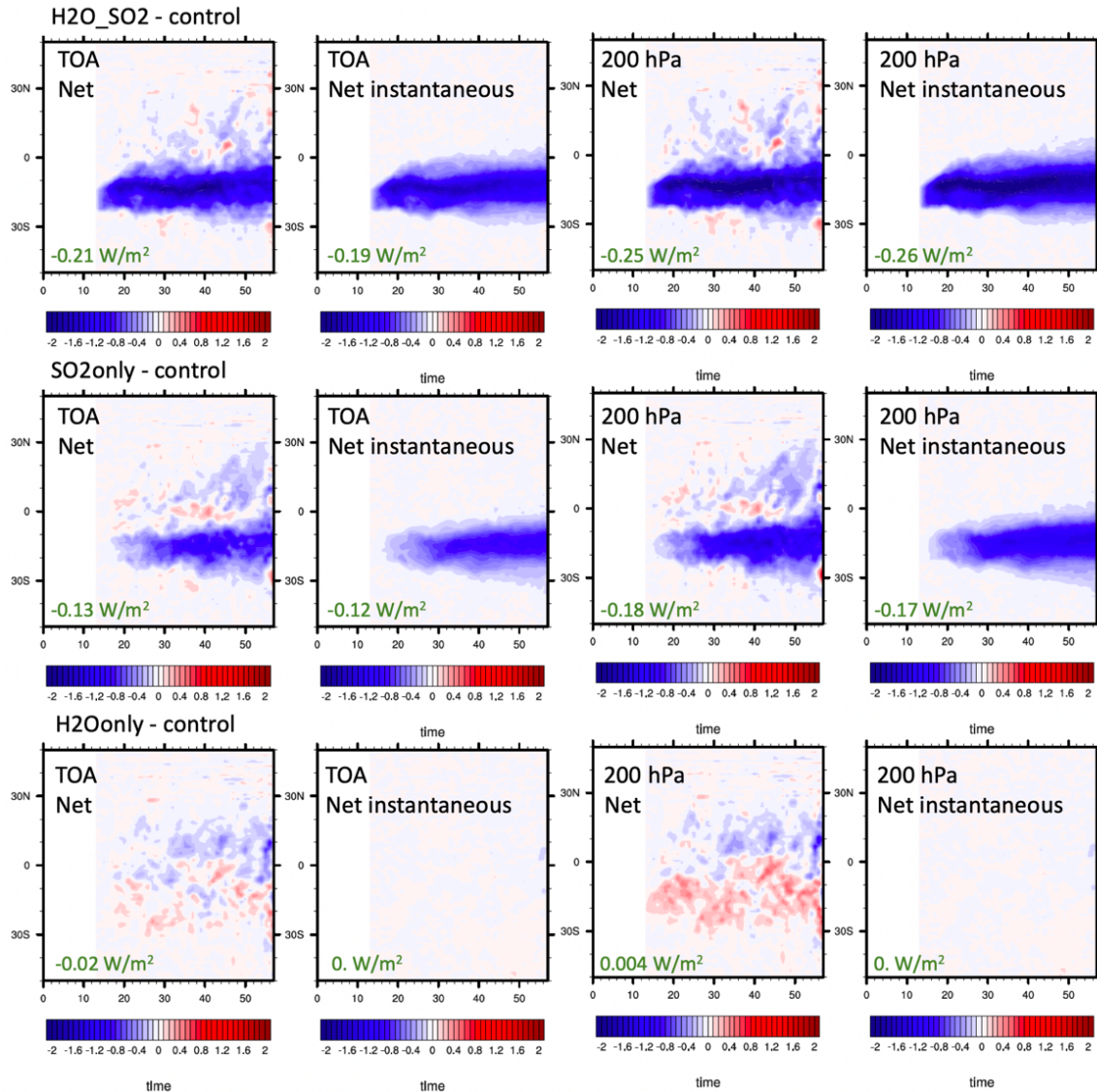


105  
106  
107  
108  
109  
110

**Supplementary Figure 8. The effective radius and weight percentage of sulfate aerosol ( $\text{SO}_4^{2-}$ : ( $\text{SO}_4^{2-} + \text{H}_2\text{O}$ ) inside the particle) comparisons between the  $\text{SO}_2\_ \text{H}_2\text{O}$  case and the  $\text{SO}_2\text{only}$  case on February 7 at 36 hPa.**



111  
 112 **Supplementary Figure 9. One of the OMPS-LP extinction profiles on March 2 compared**  
 113 **with the SO<sub>2</sub>\_H<sub>2</sub>O simulation for the same sampling.** They show a consistent vertical  
 114 extinction above 20 km. OMPS data near the tropical tropopause (black line) may be affected by  
 115 tropical cirrus clouds because this orbit data hasn't had cloud screening applied. They both show  
 116 that volcanic sulfate extends from 40°S to 10°N, but the simulation has smaller extinction values  
 117 in the northern hemisphere.  
 118

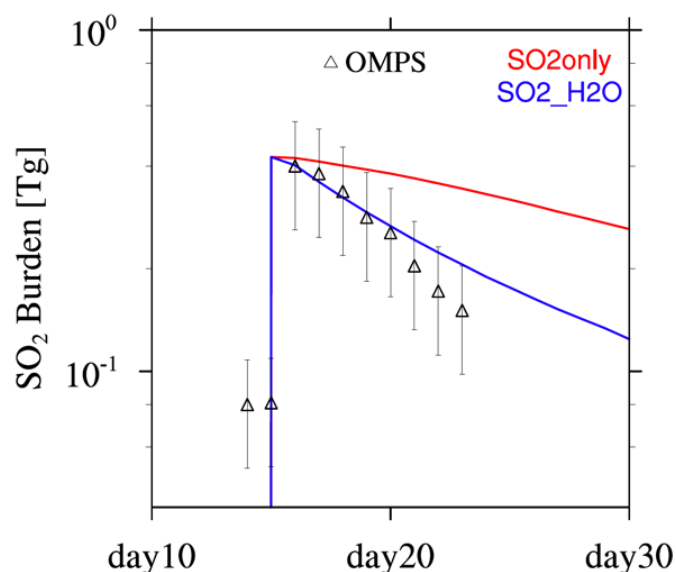


119

120 **Supplementary Figure 10. The net radiative effect anomaly from three model cases:**  
 121 **H2O\_SO2, SO2only, and H2Oonly minus control.** The first column shows the TOA adjusted  
 122 radiative effect. The second column shows the TOA instantaneous aerosol effect. The third  
 123 column shows the adjusted radiative effect at 200 hPa. The fourth column shows the  
 124 instantaneous aerosol effect at 200 hPa. The adjusted radiative effect includes flux changes  
 125 directly caused by a change in atmospheric composition and resulting from changing  
 126 atmospheric or surface state. The adjusted radiative effect is calculated using the clear sky (no  
 127 cloud) net flux. The instantaneous aerosol effect is calculated using the clear sky (no cloud  
 128 net flux minus the clean sky (not cloud and no aerosol) net flux. The global mean values for each  
 129 panel are marked in the bottom left corner. The instantaneous aerosol effect shows aerosol gives  
 130 negative radiative effects comparable to the adjusted radiative effect. The radiative effect from  
 131 water is positive in the Southern hemisphere but is much smaller than that of the aerosol in both  
 132 TOA and 200 hPa. Also, the global averaged radiative effect in the H2Oonly case at TOA in the  
 133 Southern hemisphere is cancelled out by the negative values in the Northern hemisphere,



134 resulting in a slightly negative global average value. The instantaneous effect is small in the  
135 H2Oonly case because no volcanic aerosol is injected.  
136



137  
138  
139 **Supplementary Figure 11. The time series of the stratospheric SO<sub>2</sub> burden similar to**  
140 **Figure 2.** The triangles are SO<sub>2</sub> measurements by OMPS-NM without applying the detection  
141 limit. The solid lines are the model simulations without applying the detection limit.  
142  
143

## 144 Data Availability

145 The supplementary data are available at (<https://osf.io/6ZXFV/>) with a permanent doi  
146 10.17605/OSF.IO/6ZXFV.

147  
148

## 149 Supplementary References

- 150 1. Gettelman, A. *et al.* The Whole Atmosphere Community Climate Model Version 6  
151 (WACCM6). *Journal of Geophysical Research: Atmospheres* **124**, 12380–12403 (2019).
- 152 2. Goff, J. & Gratch, S. Low Pressure Properties of H<sub>2</sub>O From-120F to 212F. *Heating, Piping*  
153 *and Air Conditioning* **18**, 125–136 (1946).

- 154 3. LeGrande, A. N., Tsigaridis, K. & Bauer, S. E. Role of atmospheric chemistry in the climate  
155 impacts of stratospheric volcanic injections. *Nature Geoscience* **9**, 652–655 (2016).
- 156 4. Jäger, H. & Deshler, T. Lidar backscatter to extinction, mass and area conversions for  
157 stratospheric aerosols based on midlatitude balloonborne size distribution measurements.  
158 *Geophysical Research Letters* **29**, 35–1 (2002).
- 159 5. Jäger, H. & Deshler, T. Correction to “Lidar backscatter to extinction, mass and area  
160 conversions for stratospheric aerosols based on midlatitude balloonborne size distribution  
161 measurements”. *Geophys. Res. Lett* **30**, 1382 (2003).
- 162 6. Prata, A. T., Young, S. A., Siems, S. T. & Manton, M. J. Lidar ratios of stratospheric volcanic  
163 ash and sulfate aerosols retrieved from CALIOP measurements. *Atmospheric Chemistry and  
164 Physics* **17**, 8599–8618 (2017).
- 165 7. Murphy, D. M. *et al.* Radiative and chemical implications of the size and composition of  
166 aerosol particles in the existing or modified global stratosphere. *Atmos. Chem. Phys. Discuss.*  
167 **2020**, 1–32 (2020).
- 168 8. Carn, S., Krotkov, N., Fisher, B. & Li, C. Out of the blue: volcanic SO<sub>2</sub> emissions during the  
169 2021-2022 Hunga Tonga-Hunga Ha’apai eruptions. *Front. Earth Sci.* (2022)  
170 doi:10.3389/feart.2022.976962.
- 171 9. Zhu, Y. *et al.* Persisting volcanic ash particles impact stratospheric SO<sub>2</sub> lifetime and aerosol  
172 optical properties. *Nature Communications* **11**, 4526 (2020).

173